al velocity in the lowest 3 km is $\lesssim 4$ cm sec^{-1}. This is small compared to the ~ 10 m sec^{-1} of zonal winds higher in the troposphere that have been inferred from the thermal wind relation (*14*). Moreover, organized vertical motions are probably required to effect the necessary precipitation; longitudinal structure indicative of such motions is not readily apparent in Voyager imaging or infrared data (*14, 22*).

Sagan and Dermott (*8*) argued that the presence of large land masses precludes the existence of a global ocean. The land would act as a barrier to the tidal flow of the ocean and generate too much dissipation to be consistent with the high eccentricity of Titan's present orbit. From a geological viewpoint, Titan is unlikely to possess a network of ocean basins and continents because the satellite is too small to generate any large amount of tectonic activity, and it is too far from Saturn for tidal dissipation to be very significant. This is consistent with the low relief observed on other large, icy, inactive bodies, such as Ganymede and Callisto (*23*). Thus, if oceans are absent at two locations on Titan, they may be absent everywhere.

Note added in proof: The analysis presented here was applied to methane oceans. Some of the heavier hydrocarbons produced by methane dissociation in the upper atmosphere, such as ethane and propane, are readily soluble in liquid methane, and, in bulk concentrations, could depress the methane vapor pressure at the surface. The nature and likelihood of such hydrocarbon oceans are currently under study.

F. M. FLASAR

Laboratory for Extraterrestrial Physics, NASA/Goddard Space Flight Center, Greenbelt, Maryland 20771

References and Notes

1. G. L. Tyler, V. R. Eshelman, J. D. Anderson, G. S. Levy, G. F. Lindal, G. E. Wood, T. A. Croft, *Science* **212**, 201 (1981).
2. R. A. Hanel *et al.*, *ibid.*, p. 192.
3. G. P. Kuiper, *Astrophys. J.* **100**, 378 (1944).
4. D. F. Strobel, *Planet. Space Sci.* **30**, 839 (1982).
5. R. E. Samuelson, R. A. Hanel, V. G. Kunde, W. C. Maguire, *Nature (London)* **292**, 688 (1981).
6. R. Courtin, *Icarus* **51**, 466 (1982).
7. T. Owen, *Sci. Am.* **246**, 98 (February 1982).
8. C. Sagan and S. F. Dermott, *Nature (London)* **300**, 731 (1982).
9. R. E. Samuelson, *Icarus* **53**, 364 (1983).
10. E. Augstein, in *Meterology over the Tropical Oceans*, D. B. Shaw, Ed. (Royal Meteorological Society, London, 1978), p. 73.
11. R. D. Goodwin, *J. Res. Natl. Bur. Stand. Sect. A* **75**, 15 (1971).
12. S. Angus, B. Armstrong, K. M. de Reuck, *International Thermodynamic Tables of the Fluid State—5: Methane* (Pergamon, Oxford, 1976).
13. C. B. Leovy, *J. Geophys. Res.* **74**, 3313 (1969); ——— and Y. Minz, *J. Atmos. Sci.* **26**, 1167 (1969).
14. F. M. Flasar, R. E. Samuelson, B. J. Conrath, *Nature (London)* **292**, 693 (1981).
15. G. F. Lindal *et al.*, *Icarus* **53**, 348 (1983).
16. G. Fjeldbo and V. R. Eshleman, *Planet. Space Sci.* **16**, 1035 (1968).
17. T. K. Bose, J. S. Sochanski, R. H. Cole, *J. Chem. Phys.* **57**, 3592 (1972); R. H. Orcutt and R. H. Cole, *ibid.* **46**, 697 (1967); L. Essen and K. D. Froome, *Proc. Phys. Soc. London Sect. B* **64**, 862 (1951).
18. H. C. van de Hulst, *Light Scattering by Small Particles* (Wiley, New York, 1962), pp. 37 and 70; R. L. Amey and R. H. Cole, *J. Chem. Phys.* **40**, 146 (1964).
19. E. Bender, *Chem. Ing. Tech.* **44**, 576 (1972); *Cryogenics* **13**, 11 (1973); K. Bühner, G. Maurer, E. Bender, *ibid.* **21**, 157 (1981).
20. B. Ackerman, *J. Atmos. Sci.* **20**, 288 (1963); N. H. Fletcher, *The Physics of Rainclouds* (Cambridge Univ. Press, London, 1962), pp. 7–15.
21. The virtual temperature of a mixture of gas and condensate is the temperature at which dry gas (N_2) of the same pressure has the same mass density as the original mixture [D. Brunt, *Physical and Dynamical Meteorology* (Cambridge Univ. Press, London, ed. 2, 1952), pp. 31 and 41–44].
22. B. A. Smith *et al.*, *Science* **212**, 163 (1981); *ibid.* **215**, 504 (1982).
23. D. Morrison, *Annu. Rev. Astron. Astrophys.* **20**, 469 (1982).
24. I thank G. Birnbaum for providing invaluable references on dielectric constants and R. B. Stewart for providing equations of state. An anonymous reviewer suggested that methane clouds could contribute to the radio occultation refractivities. I also thank J. C. Pearl, R. E. Samuelson, B. J. Conrath, R. Hanel, J. A. Pirraglia, and C. B. Leovy for stimulating discussions and their critical reading of the manuscript.

30 November 1982; revised 28 March 1983

Venera 13 and Venera 14: Sedimentary Rocks on Venus?

Abstract. *Venera 13 and Venera 14 transmitted almost complete panoramic views of their landing sites. Analyses of the photographs show the presence of rock formations undergoing geomorphic degradation. The formations display ripple marks, thin layering, differential erosion, and curvilinear fracturings. Some of them are interpreted as lithified clastic sediments. The lithification could have taken place at depth or at the surface, resulting in a type of duricrust. The origin of the sediments is unknown but could be aeolian, volcanic, or related to impacts or to turbidity currents.*

In March 1982 the automatic landers Venera 13 and Venera 14 landed on the surface of Venus and transmitted to Earth panoramic television pictures. Preliminary determinations of the locations of the landing sites are latitude 7°30′S and longitude 303° for Venera 13 and latitude 13°15′S and longitude 310°9′ for Venera 14 (*1*). The television system was essentially an improved version of the system used in Venera 9 and Venera 10 (*2, 3*) with the difference that in Ven-

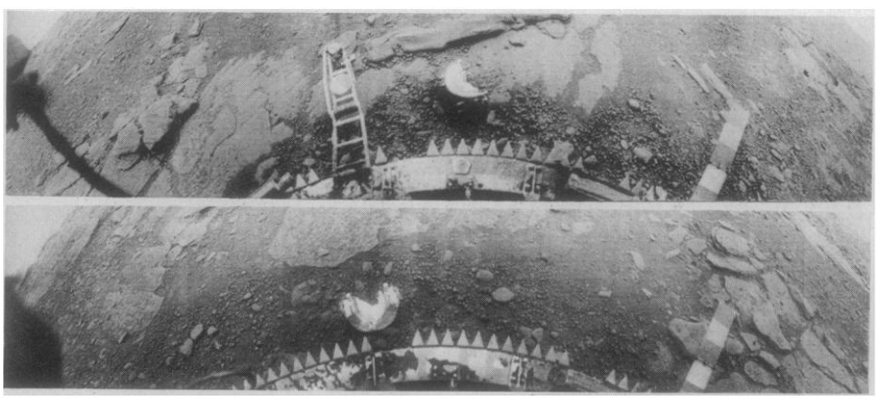

Fig. 1. Landscape photographed by Venera 13.

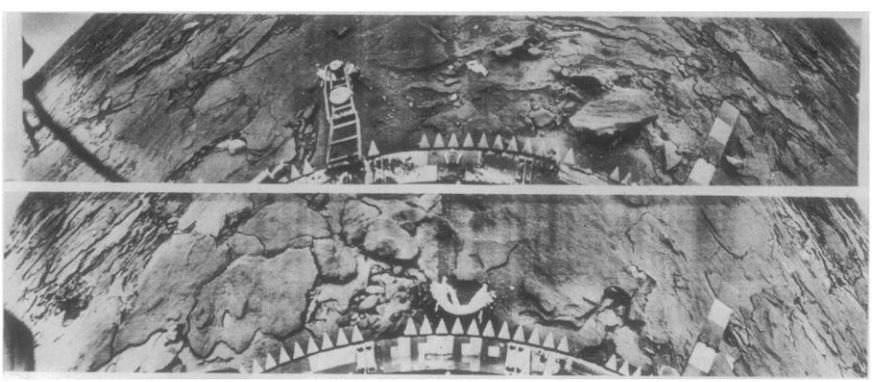

Fig. 2. Landscape photographed by Venera 14.

era 13 and Venera 14 each craft had two cameras, providing an almost complete field of view. X-ray fluorescence techniques indicate that the Venera 13 terrain is close in chemical composition to alkaline basalt and the Venera 14 terrain is close to tholeiitic basalt (*4*).

Figures 1 and 2 show the panoramas. For scale, the length of the trellis girder is 0.6 m, and the discarded viewport covers are 0.2 m in diameter and 0.12 m in height. The "eye" of the camera is 0.9 m above the ground.

Observations suggesting that some of the solid rock units are lithified loose material (here broadly referred to as sediments) are as follows. Figure 3 shows thin layers dissected by curvilinear fractures. To the left of the erosional window it is possible to see that a fracture is limited to the lower, lighter layer. Figure 4 shows alternations of light and dark striae on the surface of the slab. Perhaps this is caused by fine material accumulating in the depressions of ripple marks. Figures 5 and 6 also show striations which may be ripple marks and Fig. 6 shows the pinching out of some layers.

A sedimentary origin of the consolidated material depicted by the photographs from Venera 9 and Venera 10 was suggested (*3, 5, 6*). Venera 9 landed on a slope where slablike rocks and fine material were mass-wasting downhill. As these items have been moved and are not in situ, strictly speaking the slabs and fines are a sedimentary complex. Of more interest, however, is the origin of the slabs themselves. They are clearly the result of the breaking up of a layered structure. Some of the slabs also show the presence of layering. Venera 10 landed in a plain consisting of "islands" of consolidated outcrops in a "sea" of fine material. The outcrops are layered and there is the vague appearance of cross-bedding. The photographs from Venera 13 and Venera 14 show convincing evidence of layering. Although it is possible to produce layering by other processes, some of the characteristics of the layering strongly suggest a sedimentary origin. Specifically, these are the thin layering, the fracturing which does not cross bed boundaries, the pinching out of beds, and ripple marks. It must be stressed, however, that many of these structures could be the result of flow.

The origin of the sedimentary material is not known. Volcanism and impacts are possibilities, as are atmospheric erosion processes. Transportation could be aeolian or ballistic-aeolian. The present atmosphere is theoretically capable of aeolian transportation (*3, 5–10*). The minimum wind velocity necessary to lift particles is at least one order of magnitude smaller on Venus (about 50 cm/sec or less) than on Earth (about 600 cm/sec). Bagnold's aeolian susceptibility is almost two orders of magnitude larger on Venus than on Earth (*7*), making gentle winds capable of transportation (*11*). The absence of microdunes and ripple marks in the loose material, however, shows that extensive aeolian transportation has not occurred since lithification, at least in the areas photographed. Another possible method of transportation is by turbidity currents (*7*), perhaps triggered by impacts, volcanism, or tectonics. No graded bedding can be discerned, so the possibility that the layers are turbidites cannot be proved. No evidence is present for transportation by water (*12*). The basaltic composition of the material suggests that this is not the case, as chemical differentiation would be expected in a water environment.

Lithification of the loose material could have occurred at depth under the influence of loading pressure and increased temperature. In the present environment, the lack of water (and presumably ground water) would make lithification a different process than that on Earth. On the after hand, it is possible that the lithification was a surface-related phenomenon, so that the consolidated rocks would be a type of duricrust. If surface material is not in chemical equilibrium with the atmosphere, a process that could be called surface metamorphism may occur. Possible chemical events were discussed in (*5*). Vertical movements are necessary, either of the transported material or of air masses, perhaps caused by volcanism or impacts.

Note added in proof: The hypothesis that the layered formations are lithified sediments is strengthened by the new mechanical data: bearing strength is minimal (a few kilograms per square centimeter), density is less than 1.5 g/cm^3, and porosity is very high (as much as 50 percent).

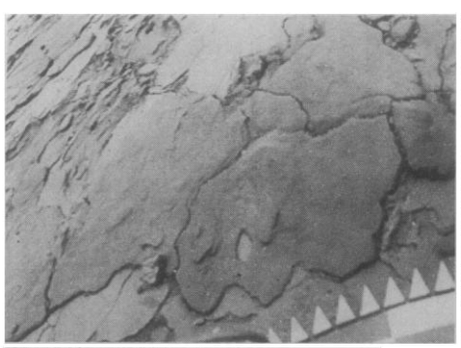

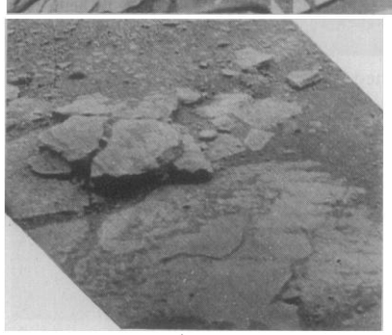

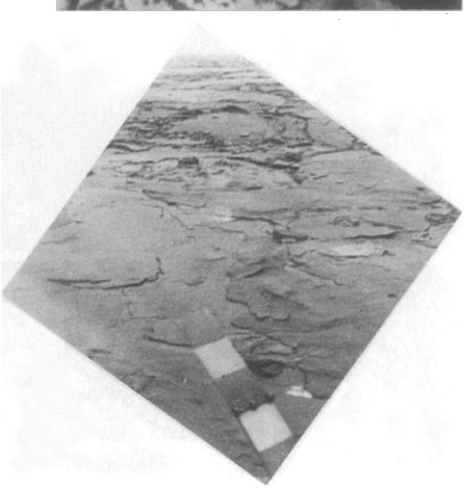

Fig. 3 (upper left). Detail of Venera 14 photograph. Fig. 4 (upper right). Detail of Venera 13 photograph. Fig. 5 (lower left). Detail of Venera 13 photograph. Fig. 6 (lower right). Detail of Venera 14 photograph.

C. P. Florensky*
A. T. Basilevsky, V. P. Kryuchkov
R. O. Kusmin, O. V. Nikolaeva
A. A. Pronin, I. M. Chernaya
Vernadsky Institute, U.S.S.R. Academy of Sciences, Moscow
Yu. S. Tyuflin
Central Scientific Research Institute of Geodesy, Moscow
A. S. Selivanov
M. K. Naraeva
State Scientific Research Center for the Study of Natural Resources, Moscow
L. B. Ronca†
Department of Geology, Wayne State University, Detroit, Michigan 48202

References and Notes

1. TASS Information, *Pravda*, 2 and 6 March 1982 (in Russian).
2. A. S. Selivanov *et al.*, *First Panoramas of the Venus Surface* (Nauka, Moscow, 1979), p. 45 (in Russian).
3. C. P. Florensky *et al.*, *Bull. Geol. Soc. Am.* **88**, 1537 (1977).
4. V. L. Barsukov, Yu. A. Surkov, L. P. Moskaleva, *Geokhimiya* **7** (1982) (in Russian), p. 72.
5. C. P. Florensky, A. T. Basilevsky, G. A. Burba, O. V. Nikolaeva, A. A. Pronin, V. P. Volkov, L. B. Ronca, *Proc. 8th Lunar Sci. Conf.* (1977), p. 2655.
6. C. P. Florensky, L. B. Ronca, A. T. Basilevsky, *Science* **196**, 869 (1977).
7. L. B. Ronca and R. R. Green, *Astrophys. Space Sci.* **8**, 59 (1970).
8. J. D. Iversen, R. Greeley, J. B. Pollack, *J. Atmos. Sci.* **33**, 2425 (1980).
9. S. L. Hess, *ibid.* **32**, 1076 (1975).
10. R. Greely *et al.*, *NASA Tech. Memo. 82385* (1980), p. 275.
11. V. S. Avduevsky *et al.*, *Kosm. Issled.* **14**, 710 (1976) (in Russian).
12. T. M. Donahue, J. H. Hoffman, R. R. Hodges, Jr., A. J. Watson, *Science* **216**, 630 (1982).

* Deceased.

† L.B.R. was at the Vernadsky Institute as a National Academy of Sciences exchange scientist.

22 September 1982; revised 18 January 1983

Requirement for Signal Peptide Cleavage of *Escherichia coli* Prolipoprotein

Abstract. *Oligonucleotide-directed site-specific mutagenesis was applied to alter the cleavage site in the signal peptide of the major outer membrane lipoprotein of* Escherichia coli. *Replacing the glycine residue at the cleavage site with an alanine residue did not affect the processing of the signal peptide. However, when the same cleavage site was constructed by the deletion of the glycine residue, the signal peptide was no longer cleaved. These results indicate that stringent structural integrity at the cleavage site in the lipoprotein signal sequence is required for correct processing of prolipoprotein.*

Secretory proteins are initially synthesized in the cytoplasm as higher molecular weight precursors that contain an extra peptide extension (signal sequence) at their amino terminals (*1*). In contrast to eukaryotic signal peptides, prokaryotic signal peptides show several major structural homologies including (i) one to three basic amino acid residues at the amino terminal, (ii) a sequence of 10 to 15 hydrophobic amino acids directly following the positively charged amino terminus, (iii) a serine or threonine residue (or both) following the hydrophobic core and located close to the carboxyl terminal, (iv) an alanine or glycine residue at the signal peptide cleavage site, and (v) in most signal peptides, a proline or glycine residue within the hydrophobic domain (*1, 2*). These common features were incorporated in a model (loop model) originally proposed to explain the functions of the signal peptide (*1, 3*). We have investigated the structural requirements at the signal peptide cleavage site of the precursor of the major outer membrane lipoprotein, the prolipoprotein, of *Escherichia coli*.

The prolipoprotein signal peptide consists of 20 amino acid residues with the sequence

```
1                   5
Met-Lys-Ala-Thr-Lys-Leu-Val-
          10                  15
Leu-Gly-Ala-Val-Ile-Leu-Gly-Ser-
                  20 ↓ 21
Thr-Leu-Leu-Ala-Gly-Cys-
```

where an arrow indicates the position of the cleavage site (*3, 4*). The positively charged amino terminal region plays an important role in efficient protein secretion across the cytoplasmic membrane (*2, 5*). We demonstrated earlier that the cleavage of the signal peptide was completely blocked if a glycine residue replaced the cysteine residue (*6*), indicating that the cysteine residue is essential for the signal peptide to be cleaved by the prolipoprotein signal peptidase (*7*). Because all prolipoproteins so far characterized have a glycine residue at the cleavage site (*2*), we examined whether the prolipoprotein signal peptidase can catalyze the cleavage of the linkage between the alanine and cysteine residues instead of the linkage between glycine and cysteine. This was achieved both by replacing the glycine residue at position 20 with an alanine residue and by deleting the same glycine residue. In order to obtain such mutations, we guided site-specific mutagenesis using as mutagens the following synthetic oligodeoxyribonucleotides (*4*).

Oligonucleotide 1:

```
5′ CTG GCA GCT TGC TCC 3′
   Leu Ala Ala Cys Ser
```

Oligonucleotide 2:

```
5′ TG CTG GCA TGC TCC AGC 3′
   Leu Leu Ala Cys Ser Ser
```

Oligonucleotide 1 is designed to cause a single base substitution in the codon for the glycine residue at the cleavage site from GGT to GCT, a codon for alanine. Oligonucleotide 2 is designed to cause a deletion of three bases GGT, the codon for the same glycine.

Guided site-specific mutagenesis was carried out as described (*2*) with the use of plasmid pMI001, a clone of the structure gene of the prolipoprotein (*5*). Five of 392 transformants after treatment with oligonucleotide 1, and 2 of 784 transformants after treatment with oligonucleotide 2, had the desired mutations. Plasmids from one of the positive colonies from each mutagenesis were further characterized by DNA sequence analysis (Fig. 1). The sequences of the mutant DNA's were identical to those predicted from the mutagenesis design. Since pMI001 had no promoter, a 0.56–kilobase (kb) Xba I–Eco RI fragment carrying the mutant *lpp* gene was isolated from each mutant plasmid and inserted into an expression cloning vector, pIN-II (*8*), which was digested with both Xba I and Eco RI. The resultant plasmids, pC_1 [pIN-II-*lpp* ($Gly^{20} \rightarrow$ Ala)] and pC_3 [pIN-II-*lpp* (ΔGly^{20})], now had the mutant *lpp* gene under the control of the *lpp* promoter and the *lac*UV5 promoter-operator (*6, 8*). Thus, the expression of the mutant *lpp* genes could be induced by a *lac* inducer such as isopropyl-β-D-thio-

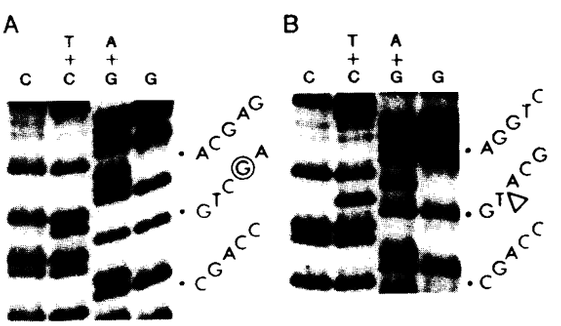

Fig. 1. DNA sequence gels corresponding to the region of the cleavage site of the prolipoprotein signal peptide of pC_1 [pIN-II-*lpp* ($Gly^{20} \rightarrow$ Ala)] and pC_3 [pIN-II-*lpp* (ΔGly^{20})]. The plasmid DNA was digested with Xba I at the unique Xba I site in the ribosome-binding site of the *lpp* gene and labeled with deoxynucleotide [^{32}P]triphosphate (*5*). The labeled DNA was cleaved with Hinf I and the approximately 120-base pair Xba I–Hinf I fragment was purified and used for sequencing (*14*). The cleavage products were applied to a 10 percent polyacrylamide gel and separated by electrophoresis. Only the region around the signal peptide cleavage site is shown. The sequences at the side of the gel are complementary to the sense sequence. The circled base indicates the base that is different from the wild-type *lpp* gene. A triangle indicates a deletion of a sequence of the three bases CCA. (A) pC_1 DNA and (B) pC_3 DNA.